Appl. Phys. A 78, 539–542 (2004)
DOI: 10.1007/s00339-003-2391-2

Applied Physics A
Materials Science & Processing

J.Y. LAO[1]
J.Y. HUANG[1]
D.Z. WANG[1]
Z.F. REN[1,✉]
D. STEEVES[2]
B. KIMBALL[2]
W. PORTER[2]

ZnO nanowalls

[1] Department of Physics, Boston College, Chestnut Hill, Massachusetts 02467, USA
[2] The US Army Natick Soldier Systems Center, Natick, Massachusetts 01760, USA

Received: 18 September 2003/Accepted: 29 September 2003
Published online: 21 November 2003 •

ABSTRACT Wurtzite ZnO nanowall structures have been synthesized on a (110) Al_2O_3 substrate by a thermal evaporation and condensation method. The nanowalls are connected to each other and have a thickness of about 20–100 nm. An excellent epitaxial relationship with the substrate has been observed by X-ray diffraction. Edge-dislocation dipoles were observed by transmission electron microscopy. Photoluminescence measurements show strong UV emission at 390 nm for the white-gray nanowalls grown at high temperature, and very weak UV emission for the reddish nanowalls grown at low temperature.

PACS 78.55.-m; 81.05.Je; 81.10.Bk; 81.15.Ef

Nanoscaled materials have attracted a great deal of interest. Recent efforts have been shifted to the synthesis, characterization and potential applications of various wide band gap semiconductor nanowires. Many semiconductor nanowires and nanorods, including Si [1, 2], Ge [3], GaN [4], GaAs [5], InAs [6], etc., have been fabricated for various potential applications. ZnO, with a wide direct band gap of 3.37 eV and a high exciton binding energy of 60 meV, which is much higher than those of ZnS (20 meV) and GaN (21 meV), is of much interest for blue and ultra-violet (UV) optical devices, transparent conductive films, solar cells [7], sensors [8, 9], photocatalysis [10], transparent field-effect transistors [11] and bulk acoustic wave devices [12]. Various ZnO nanostructures, such as nanowires [13], nanobelts [14], tetrapods [15], nanobridges and nanonails [16], and hierarchical nanostructures [17] have been synthesized. ZnO nanostructure properties and applications [18–20] have been explored. Here we report a new ZnO nanostructure: nanowalls, synthesized by the vapor–liquid–solid (VLS) method that have a morphology close to the carbon nanowall structures [21]. (We noticed a short report of a similar structure [22] when we were writing this paper.) These nanowall structures are epitaxially grown on a sapphire substrate and closely related to each other. They can be potentially used for photocatalysts, optoelectronics and templates for forming other nanowall structures using a coating [23] or nanoshells following the coating with thermal evaporation and reduction steps [24].

The ZnO nanowall is synthesized by the same thermal evaporation and condensation method as described in previous reports [16, 17, 25] except that a thin layer of gold was coated on the substrate as catalyst. No growth has been found on the catalyst-free substrate surface. Briefly, a mixture of ZnO and graphite powders was used as the source and put into the sealed end of a small quartz tube. A (110) sapphire substrate, coated with 1–3 nm of Au thin film, was placed at the open end of the quartz tube for the ZnO nanowall growth. When the substrate temperature is at about 875–950 °C and the pressure at 0.5 to 1.5 Torr air, we found ZnO nanowall structures on the sapphire substrate. The nanowalls grown at high temperature show a milky white-gray color, while the structures grown at low temperature show a reddish color.

Based on scanning electron microscopy (SEM) and X-ray diffraction (XRD) examination, not much difference has been found between the nanowalls grown at high and low temperatures. Figure 1 shows the typical SEM image of ZnO nanowall structures at 950 °C. The nanowalls interconnect with each other to form a network. The pore size varies from several hundred nanometers to 1 micron. Figure 1a shows the medium-magnification view of small nanowalls and Fig. 1b shows large-size nanowalls. Figure 1c shows the SEM image of the nanowalls with nanowires on the junctions. These nanowires are perpendicular to the substrate. Most of the nanowall flakes are perpendicular to the substrate, although some could form certain small angles with the substrate. These nanowall flakes do not exhibit a clearly ordered pattern and some pieces are curved. Nevertheless, many of the nanowall flakes are parallel to each other and show a quasi-hexagonal pattern and most of the flakes form angles that are multiples of 30°. Figure 2 shows the XRD 2-theta diffraction pattern of the white-gray nanowalls. Due to the good epitaxial relation between the *c* plane of ZnO nanowalls and the *a* plane of sapphire, only the ZnO (0002) and (0004) peaks can be seen. Figure 2b shows the Omega scan of the (0002)

✉ Fax: +1-617/552-8478, E-mail: renzh@bc.edu

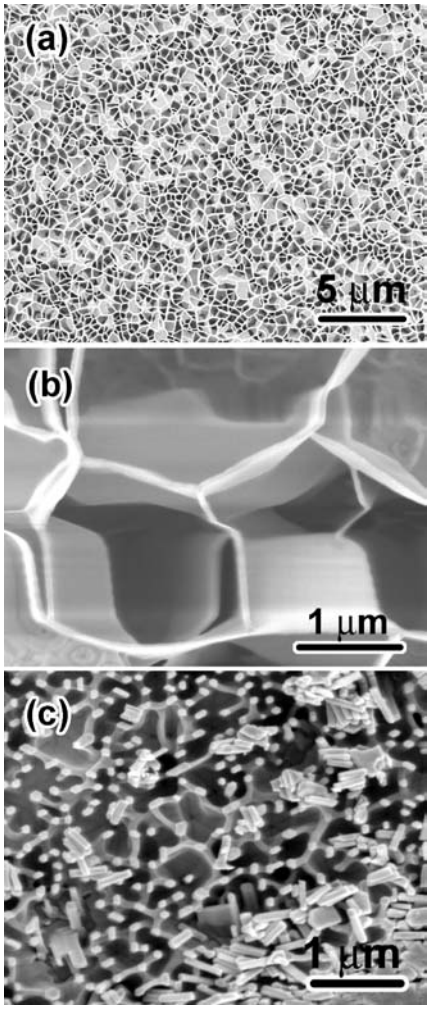

FIGURE 1 SEM images of the ZnO nanowalls synthesized by vapor transport and condensation method. **a** A medium-magnification SEM image of the small-size nanowalls. **b** A medium-magnification SEM image of the large-size nanowalls. **c** A medium-magnification SEM image of the nanowalls with nanowires at the junctions

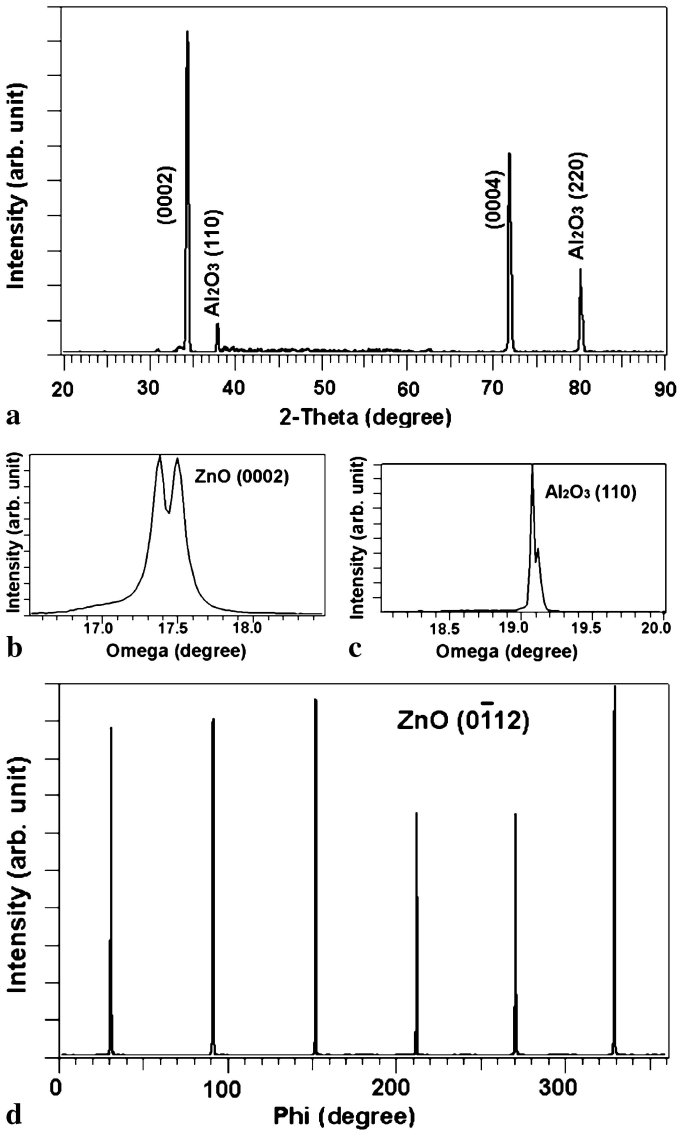

FIGURE 2 XRD spectra of the nanowalls structure. **a** 2-theta scan. **b** and **c** Omega scan of the nanowalls and substrate, respectively. **d** Phi scan of the ZnO nanowalls

peak of the sample. The peak splits into two small ones. The FWHM of the peak is 0.24 degree. The peak split has also been found from the substrate (with FWHM of 0.03 degree as shown in Fig. 2c). Therefore, the ZnO nanowall peak split is probably due to the substrate peak split. Figure 2d shows the Phi scan of the $(0\bar{1}12)$ peak of ZnO nanowalls on sapphire. The six peaks, with equivalent distance of 60 degrees, demonstrate the in-plane epitaxial relation of ZnO nanowalls with the *a*-plane single-crystal sapphire substrate.

Figure 3a shows the transmission electron microscopy (TEM) image of a ZnO nanowall flake. This nanowall flake has a width of 330 nm and a length of 800 nm. The orientation of the flake changes slightly from region to region, which is possibly caused by bending of the flake. Figure 3b shows the associated selected-area electron-diffraction (SAD) pattern. The appearance of the extinction diffraction spots such as (0001), (0003), etc., is caused by double diffraction. From the SAD pattern, the nanowall flake should be on the $\{11\bar{2}0\}$ plane, and the direction from bottom to top of the paper is [0001]. This result is consistent with the XRD result shown in Fig. 2a. Interestingly, the two long edges (indicated by arrows) of the nanowalls are on the high-index plane inclined to the (0002) plane, and they are composed of many steps of small (0002) facets. Figure 3c shows a higher-magnification phase-contrast image clearly showing the dislocations in the flake. Lots of the nanowall flakes have such dislocations. Figure 3d shows the high-resolution TEM image of the flake. These dislocations with a length of about 20 nm distribute periodically in the flake. A high-resolution image such as that shown in Fig. 3d indicates that each dislocation line is associated with two heavily strained areas. If one draws a Burgers circuit to enclose each heavily strained area (Fig. 3d), one can see that each strained area is associated with a perfect dislocation with a Burgers vector of either $1/3\,[2\bar{1}\bar{1}0]$ or $1/3\,[\bar{2}110]$. The fact that each dislocation line is associated with two dislocations with opposite Burgers vectors suggests that these dislocations are actually disloca-

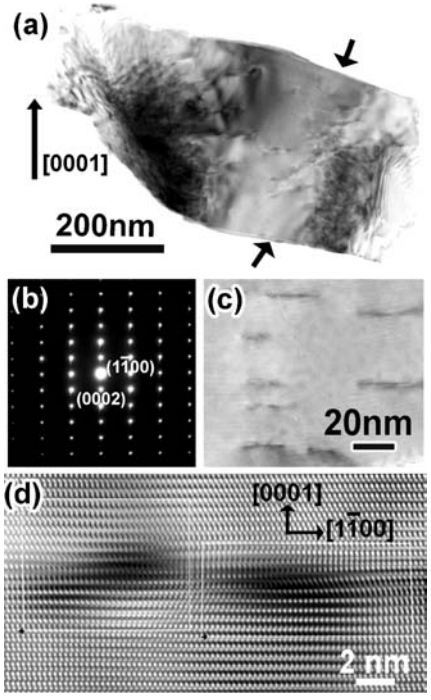

FIGURE 3 TEM micrographs of the nanowalls structure. **a** A low-magnification TEM image of a nanowall flake. **b** A SAD pattern. **c** A high-magnification phase-contrast image showing the edge-dislocation dipoles. **d** A high-resolution TEM image of the dislocation dipole

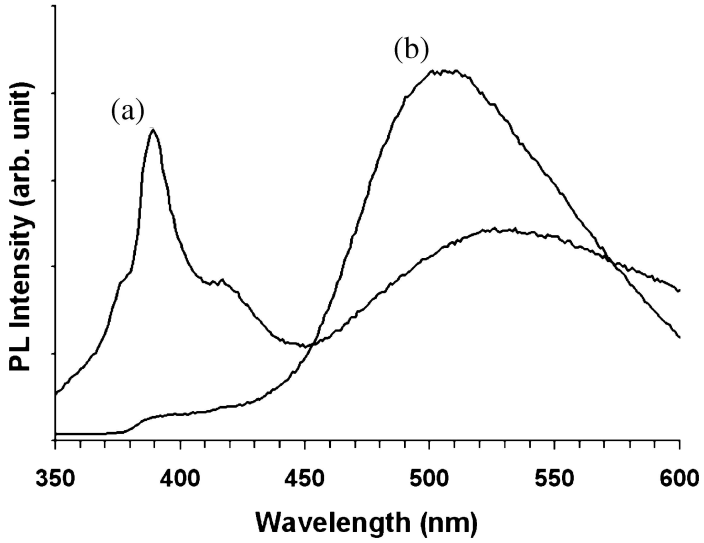

FIGURE 4 Photoluminescence spectra of the nanowalls. **a** Spectrum of white-gray nanowalls grown at high temperature and **b** spectrum of reddish nanowalls grown at low temperature

tion dipoles. The Burgers vectors of these perfect dislocations are parallel to the (0002) plane, which are typical mobile dislocations in a hexagonal structure. The reason for the existence of dislocations in the flakes is not clear.

We have also managed to grow aligned ZnO nanowire arrays on *a*-plane sapphire substrates using a similar method. Au catalyst is also necessary to grow the aligned nanowires with either white-gray or reddish color, the same as for nanowall growth. Therefore, the growth of the nanowalls must be based on the VLS mechanism. During the nucleation and growth stage, the Au−Zn alloy on the substrate surface could form connected ripples instead of the separated dots that are the formation bases for the aligned arrays. The subsequent deposition of Zn vapor and oxidation of segregated Zn from supersaturated Au−Zn alloy results in the nanowall structure. Due to the epitaxy of the nanowalls to the sapphire substrate, the nanowalls are both in-plane and out-of-plane aligned.

For photoluminescence (PL) measurements, the samples were irradiated with an excitation wavelength of 325 nm and emission scanning was performed in the range 340–600 nm. Figure 4 shows the room-temperature photoluminescence measured on as-prepared ZnO nanowalls on a sapphire substrate. Curve (a) is the spectrum from white-gray nanowalls grown at higher temperature, and curve (b) is that from reddish nanowalls grown at lower temperature. The strong UV emission at 390 nm for spectrum (a) is attributed to the band-edge emission of ZnO wurtzite structure. The green-yellow broad deep-level emission is not as strong. Spectrum (b) shows big broad green-yellow emissions, but very weak UV emission. The broad green-yellow emission band is attributed to a defect that results in radiative transitions between shallow donors and deep acceptors [26]. Vanheusden et al. [27] proved that the green-yellow luminescence is due to the single oxygen vacancy in ZnO and the radiative combination of a photogenerated hole with an electron occupying the oxygen vacancy. These results are consistent with other reports [28]. No obvious quantum-effect shift has been found for the spectrum compared to the bulk, which is understandable because usually the structure needs to be smaller than 20 nm to show the quantum effect. Annealing can also change the spectrum. Annealing in oxygen atmosphere at 600 °C for 2 h suppresses the green-yellow emission completely, and a vacuum annealing at 400 °C suppresses both the UV and the green-yellow emissions by a small amount. The strong emission from the band edge suggests the excellent crystalline structure of the nanowalls grown at high temperature.

In conclusion, we have synthesized ZnO nanowall structures on an *a*-plane sapphire substrate. The nanowall grows epitaxially from the substrate. Growth temperature has an effect on the nanowalls' color and photoluminescence emission. Oxygen and vacuum annealing also change the PL spectra. The same structure has not been grown on a Si substrate under the same conditions because the epitaxy relation is necessary for the nanowall growth.

ACKNOWLEDGEMENTS The authors would like to thank W.Z. Li and Y. Tu for helpful discussions. This work is supported partly by the US Army Natick Soldier Systems Center under Grant Nos. DAAD16-03-C-0052 and DAAD16-00-C-9227, partly by the DOE under Grant No. DE-FG02-00ER45805 and partly by the NSF under Grant No. CMS-0219826.

REFERENCES

1 A.M. Morales, C.M. Lieber: Science **279**, 208 (1998)
2 W.S. Shi, H.Y. Peng, N. Wang, C.P. Li, L. Xu, C.S. Lee, R. Kalish, S.-T. Lee: J. Am. Chem. Soc. **123**, 11 095 (2001)
3 Y. Wu, P.D. Yang: Chem. Mater. **12**, 605 (2000)
4 W. Han, S. Fan, Q. Li, Y. Hu: Science **277**, 1287 (1997)
5 J. Hu, T.W. Odom, C.M. Lieber: Acc. Chem. Res. **32**, 435 (1999)
6 M. Yazawa, M. Koguchi, A. Muto, M. Ozawa, K. Hiruma: Appl. Phys. Lett. **61**, 2051 (1992)
7 K. Hara, T. Horiguchi, T. Kinoshita, K. Sayama, H. Sugihara, H. Arakawa: Sol. Energy Mater. Sol. Cells **64**, 115 (2000)

8 G. Sberveglieri, S. Groppelli, P. Nelli, A. Tintinelli, G. Giunta: Sens. Actuators B **25**, 588 (1995)
9 J.A. Rodriguez, T. Jirsak, J. Dvorak, S. Sambasivan, D. Fischer: J. Phys. Chem. B **104**, 319 (2000)
10 H. Yumoto, T. Inoue, S.J. Li, T. Sako, K. Nishiyama: Thin Solid Films **345**, 38 (1999)
11 P.F. Carcia, R.S. McLean, M.H. Reilly, G. Nunes, Jr.: Appl. Phys. Lett. **82**, 1117 (2003)
12 B.S. Panwar: Appl. Phys. Lett. **80**, 1832 (2002)
13 M.J. Zheng, L.D. Zhang, G.H. Li, W.Z. Shen: Chem. Phys. Lett. **363**, 123 (2002)
14 Z.W. Pan, Z.R. Dai, Z.L. Wang: Science **291**, 1947 (2001)
15 Y. Li, G.W. Meng, L.D. Zhang, F. Phillipp: Appl. Phys. Lett. **76**, 2011 (2000)
16 J.Y. Lao, J.Y. Huang, D.Z. Wang, Z.F. Ren: Nano Lett. **3**, 235 (2003)
17 J.Y. Lao, J.G. Wen, Z.F. Ren: Nano Lett. **2**, 1287 (2002)
18 M.H. Huang, S. Mao, H. Feick, H.Q. Yan, Y.Y. Wu, H. Kind, E. Weber, R. Russo, P.D. Yang: Science **292**, 1897 (2001)
19 C.J. Lee, T.J. Lee, S.C. Lyu, Y. Zhang, H. Ruh, H.J. Lee: Appl. Phys. Lett. **81**, 3648 (2002)
20 H.T. Ng, B. Chen, J. Li, J. Han, M. Meyyappan, J. Wu, S.X. Li, E.E. Haller: Appl. Phys. Lett. **82**, 2023 (2003)
21 Y.H. Wu, P.W. Qiao, T.W. Chong, Z.X. Shen: Adv. Mater. **14**, 64 (2002)
22 H.T. Ng, J. Li, M. Smith, P. Nguyen, A. Cassell, J. Han, M. Meyyappan: Science **300**, 1249 (2003)
23 Y.H. Wu, B. Yang, G. Han, B. Zong, H. Ni, P. Luo, T. Chong, T. Low, Z. Shen: Adv. Funct. Mater. **12**, 489 (2002)
24 J. Goldberger, R. He, Y. Zhang, S. Lee, H. Yan, H. Choi, P.D. Yang: Nature **422**, 599 (2003)
25 J.Y. Lao, J.G. Wen, D.Z. Wang, Z.F. Ren: Int. J. Nanosci. **2**, 149 (2002)
26 H.-J. Egelhaaf, D. Oelkrug: J. Cryst. Growth **161**, 190 (1996)
27 K. Vanheusden, C.H. Seager, W.L. Warren, D.R. Tallant, J.A. Voigt: Appl. Phys. Lett. **68**, 403 (1996)
28 B.D. Yao, Y.F. Chan, N. Wang: Appl. Phys. Lett. **81**, 757 (2002)